

Supporting Information

Dual-shell microcapsules for high-response efficiency self-healing of multi-scale damage in waterborne polymer-cement coatings

Chenyang Liu¹, Zhicheng Sun^{1*}, Shouzheng Jiao², Ting Wang¹, Yibin Liu¹, Xianyu Meng³, Binbin Zhang³, Lu Han¹, Ruping Liu¹, Yuanyuan Liu⁴, Yang Zhou^{4*}

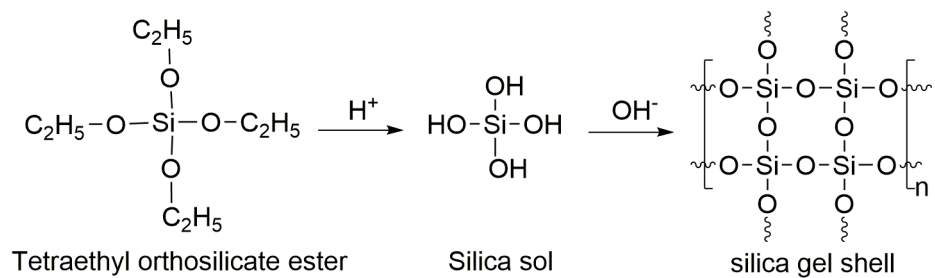


Figure S1 Reaction formula for silica gel shell preparation

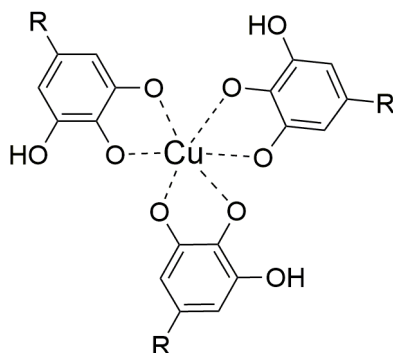


Figure S2 Structural formula of TA-Cu²⁺ chelates

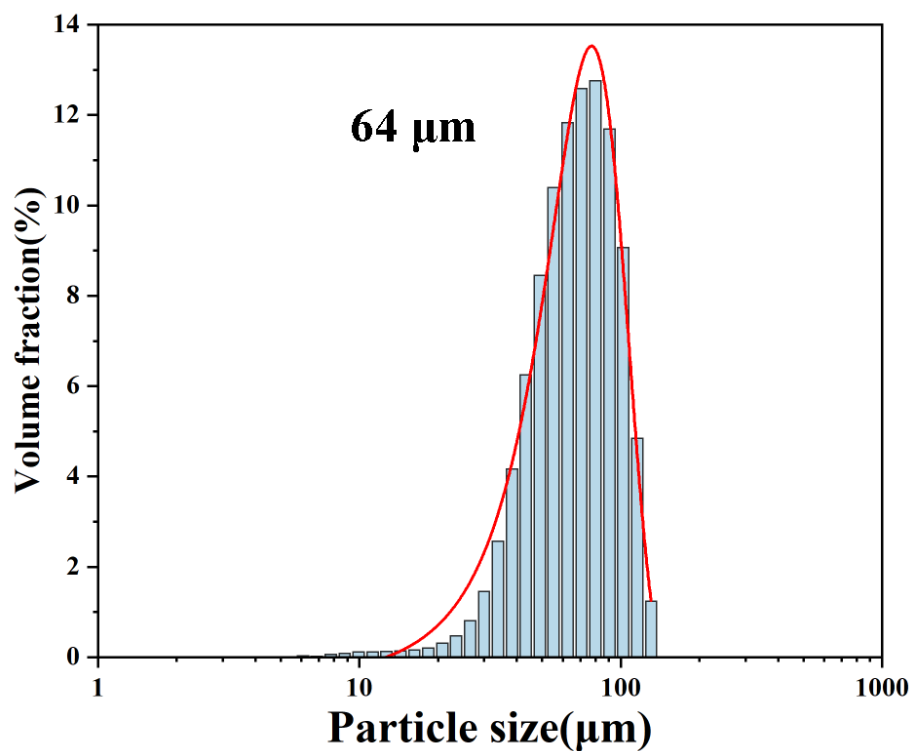


Figure S3 Particle size distributions of microcapsules

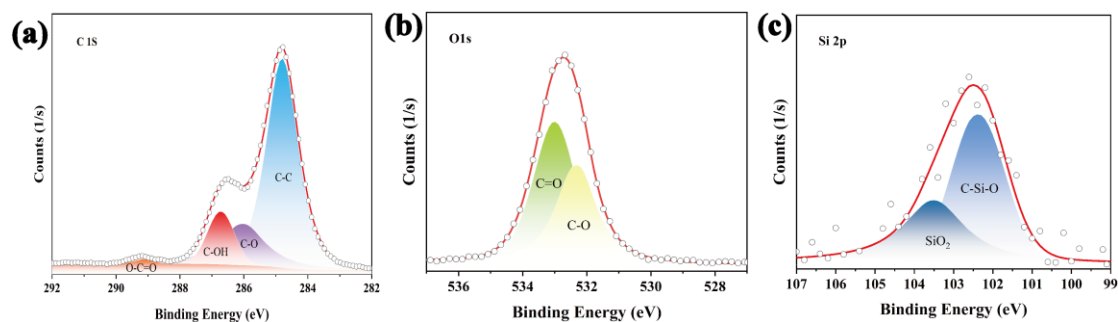


Figure S4. Self-healing microcapsules characterization by XPS analysis. (a) C1s peak was deconvoluted to 284.8, 286.7, 286 and 289 eV, corresponding to C-C, C-O-Ph, C-O-C/C-OH, and C=O functionalities in TA, respectively. (b) O1s spectrum was deconvoluted to 533.0 and 532.4 eV, representing the organic C-O and O-H structures, respectively. (c) The absorption peaks of Si2p at 102.3 and 103.5 are derived from C-Si-O and SiO₂, respectively, which further confirms the successful encapsulation of EP@SiO₂@TA-Cu bilayer shell in self-healing microcapsules.

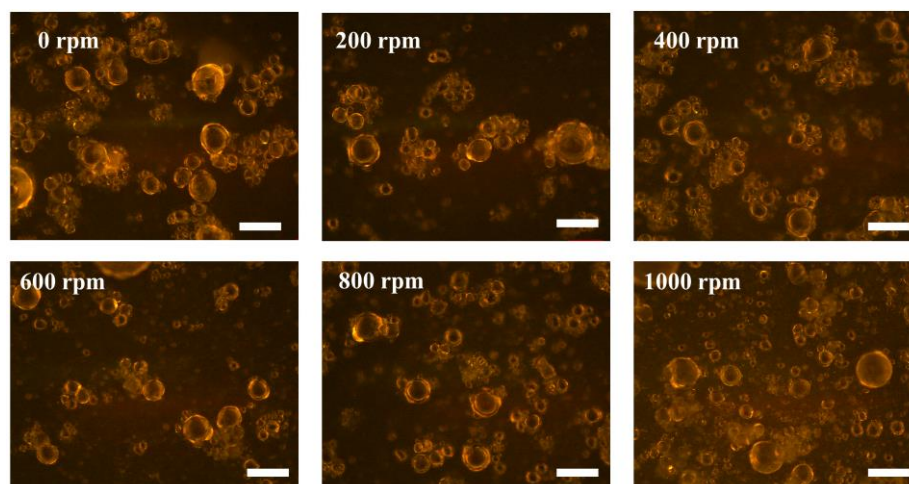


Figure S5. POM images of self-healing microcapsules in Stirring tests.

scale bar: 100 μ m

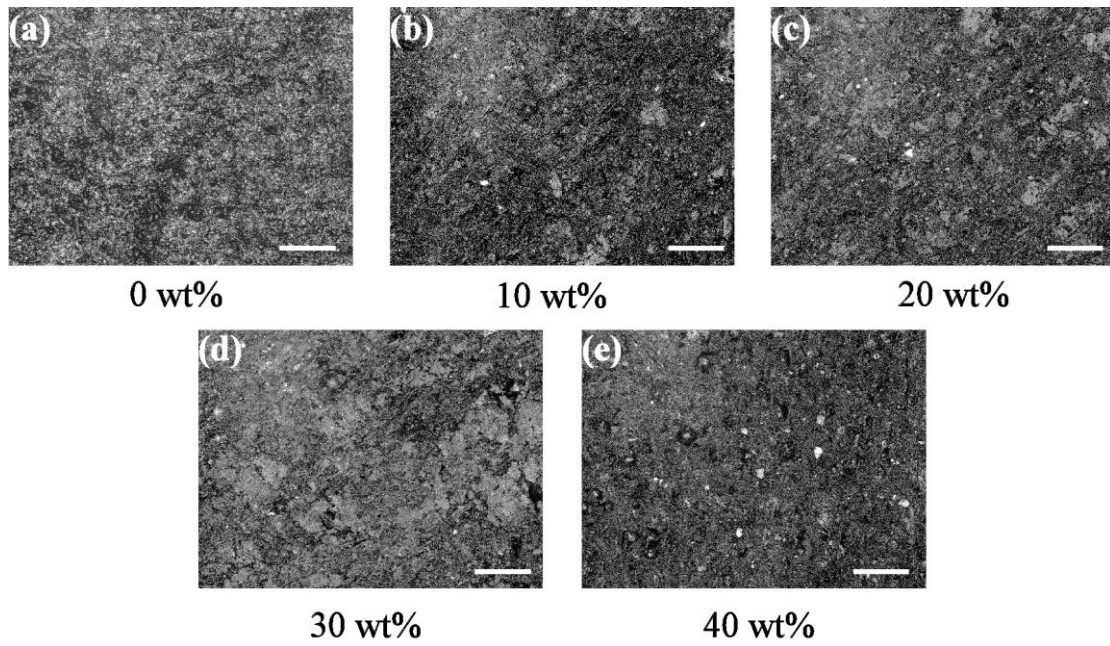


Figure S6. laser confocal microscopy images of coatings with different microencapsulates additions

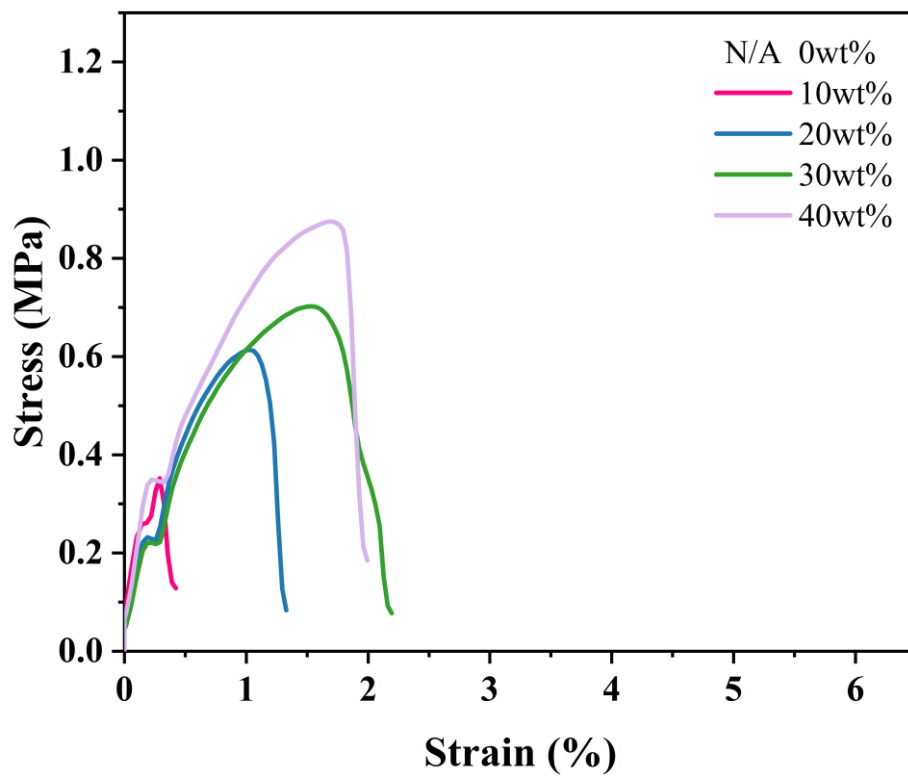


Figure S7. The tensile strength of the cut off coating after self-healings

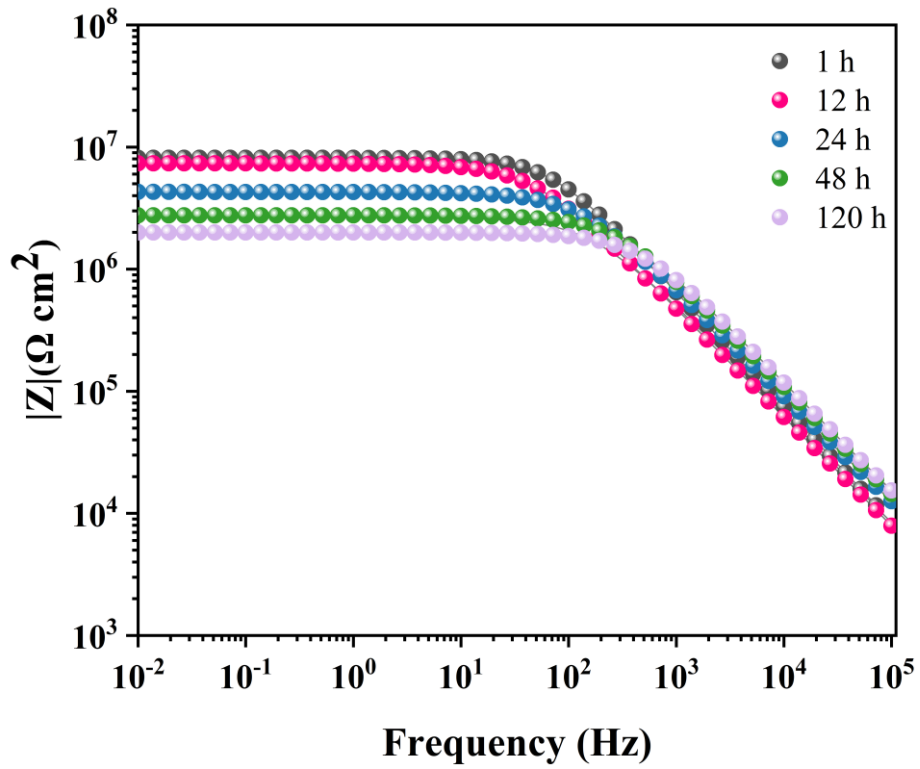


Figure S8. Bode plots of self-healing coatings with different times immersion in 3.5

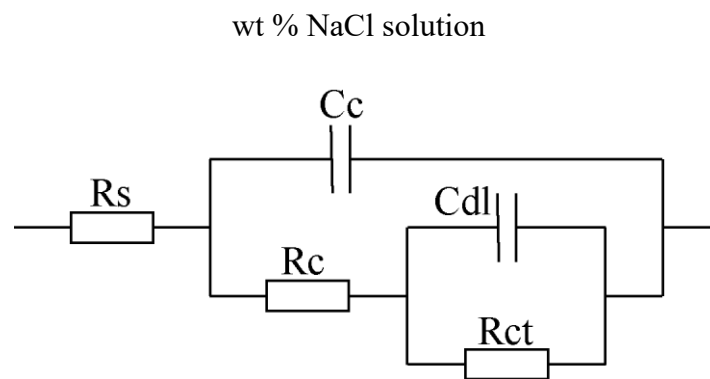


Figure S9. electrical equivalent circuits used to fit the impedance data